

# Polymer Chemistry

Accepted Manuscript



This is an *Accepted Manuscript*, which has been through the Royal Society of Chemistry peer review process and has been accepted for publication.

*Accepted Manuscripts* are published online shortly after acceptance, before technical editing, formatting and proof reading. Using this free service, authors can make their results available to the community, in citable form, before we publish the edited article. We will replace this *Accepted Manuscript* with the edited and formatted *Advance Article* as soon as it is available.

You can find more information about *Accepted Manuscripts* in the [Information for Authors](#).

Please note that technical editing may introduce minor changes to the text and/or graphics, which may alter content. The journal's standard [Terms & Conditions](#) and the [Ethical guidelines](#) still apply. In no event shall the Royal Society of Chemistry be held responsible for any errors or omissions in this *Accepted Manuscript* or any consequences arising from the use of any information it contains.

Cite this: DOI: 10.1039/c0xx00000x

www.rsc.org/xxxxxx

ARTICLE TYPE

# Synthesis of Water Soluble Polyrotaxanes by End-capping Polypseudorotaxanes of $\gamma$ -CDs with PHEMA-PPO-PEO-PPO-PHEMA Using ATRP of MPC

Tao Kong<sup>a</sup>, Jing Lin<sup>a</sup>, Lin Ye<sup>a</sup>, Ai-ying Zhang<sup>a</sup> and Zeng-guo Feng<sup>\*a</sup>

Received (in XXX, XXX) Xth XXXXXXXXX 20XX, Accepted Xth XXXXXXXXX 20XX  
DOI: 10.1039/b000000x

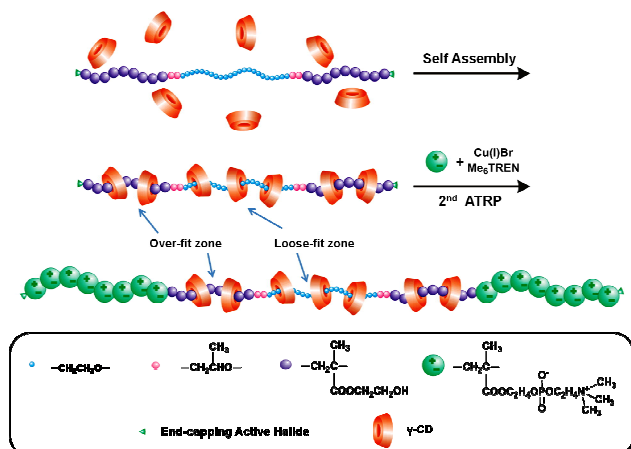
A twice ATRP protocol is developed for the preparation of water soluble single-chain stranded polyrotaxanes (PRs) by end-capping polypseudorotaxanes (PPRs) formed from  $\gamma$ -CDs with PHEMA-PPO-PEO-PPO-PHEMA using oligomers of MPC as bulky stopper. It is shown that those threaded  $\gamma$ -CDs simultaneously reside on PHEMA and PEG segments to give access to both loose- and over-fit structured PR-based multi-block copolymers.

Single-chain stranded cyclodextrin (CD)-based polyrotaxanes (PRs) are a family of supramolecular polymers typically prepared by end-capping polypseudorotaxanes (PPRs) self-assembled from a single polymeric chain with CD molecules via hydrogen bonding, hydrophobic and/or van der Waals host-guest interactions using bulky stoppers or oligomers<sup>1</sup>. Due to fantastically slidable and rotary entrapped CD rings<sup>2</sup>, a number of functional polymeric axles available<sup>3</sup>, hierarchical topological structures<sup>4</sup> and feasible further modifications<sup>5</sup>, these supramolecular assemblies present intriguing properties, such as stimulus-responsibility, self-healing, shape-memory, etc., and have received tremendous attention in the last decades for their fertile potential as smart materials<sup>6</sup>.

In theory, the specific recognition or size matching of CDs with a single polymeric chain and afterwards effectively end-capping the axle terminals of the resulting PPRs are two crucial factors for the synthesis of single-chain stranded  $\gamma$ -CD-based PRs<sup>7</sup>. For example,  $\gamma$ -CDs can include with PPO to form tight-fit PPRs showing a characteristic channel-like crystal structure via the size matching recognition<sup>8</sup>. However, they can hardly contain single PEG or PEA chain, instead double chains to give rise to tight-fit PPRs<sup>9,10</sup>. Recently, Yui *et al.* prepared first loose-fit single-chain stranded  $\gamma$ -CD/PEG PRs via the condensation reaction only in isolated 6 % yield<sup>11</sup>. Just as indicated by Harada *et al.*<sup>8</sup>, it is more difficult to prepare single-chain stranded PRs composing of bigger  $\gamma$ -CDs and thinner polymer chains, such as PEG and PEA by the classic recognition/threading synthetic strategy as compared with their smaller and more rigid counterparts, such as  $\alpha$ - and  $\beta$ -CDs. This unfavourable recognition is due to the mismatch of the cross-sectional area of incoming polymer chain with the cavity size of  $\gamma$ -CDs<sup>12</sup>. At the same time, the  $\gamma$ -CDs also hold a high structural deformation ability to some extent in solvents<sup>13</sup>. For instance, they can include not only PPO, but also thicker PDMS and

PMVE to produce tight-fit PPRs<sup>14,15</sup>. It is easily envisaged that the size mismatch of incoming polymer chain with the cavity of  $\gamma$ -CDs would endow PRs the unique stimuli-responsibility with regard to those  $\alpha$ - and  $\beta$ -CD ones. To this end, it is desirable to develop a highly efficient preparation technique for single-chain stranded  $\gamma$ -CD-based PRs showing the designed molecular architecture to enrich the chemistry of supramolecular polymers. In the past few years, the atom transfer radical polymerization (ATRP) has been utilized to attach oligomers as bulky stopper to transform PPRs into PRs<sup>16-18</sup>. However, taking account of more flexible conformation of  $\gamma$ -CDs, there are fewer studies devoted to the synthesis of single-chain stranded unmatched  $\gamma$ -CD-based PRs by ATRP. In a very recent article<sup>19</sup>, we report that flanking bulky PHEMA blocks attached by ATRP could change the recognition process of  $\gamma$ -CDs with PPO-PEO-PPO wherein the  $\gamma$ -CDs are threaded onto and moved over the PHEMA segments to produce  $\gamma$ -CD/PHEMA-PPO-PEO-PPO-PHEMA PPRs featured by both loose-fit (with PEO) and over-fit (with PHEMA) architectures in aqueous media, different from those  $\gamma$ -CD/PPO-PEO-PPO tight-fit single chain bent stranded PPRs exhibiting the characteristic channel-like crystal structure<sup>15</sup>. Significantly, these PPRs still preserve the active halide ends prone to be used to initiate the second ATRP so as to converse them into PRs. It would offer direct evidence to confirm the existence of loose-fit and over-fit structures in the PPRs and PRs. Herein, upon the formation of  $\gamma$ -CD/PHEMA-PPO-PEO-PPO-PHEMA PPRs, they are used as macroinitiator for the second ATRP of water-soluble 2-methacryloyloxyethyl phosphorylcholine (MPC) to transform themselves into the loose-fit and over-fit structured supramolecular polymers<sup>20-22</sup>. Their synthetic strategy is shown in Scheme 1. As described in Scheme S1, PHEMA blocks with a total average degree of polymerization (DP) equal to 26 are attached to a distal 2-bromoisobutryl end-capped PPO-PEO-PPO (BrPEPBr) by the first ATRP of 2-hydroxyethyl methacrylate (HEMA) to give rise to the target pentablock copolymer (PEP26H) followed by self-assembly with  $\gamma$ -CDs to construct unique  $\gamma$ -CD/PHEMA-PPO-PEO-PPO-PHEMA PPRs exhibiting both single-chain stranded loose-fit and over-fit structure. For a possible hydrolytic reaction of end-capped bromine in the first aqueous ATRP of HEMA which could reduce the chain end functionality and efficiency of second ATRP as previously reported<sup>23</sup>, Cu(I)Cl/PMDETA is chosen as catalyst and DMF is used as solvent for the first ATRP

in this study<sup>24</sup>. Furthermore, the crude PEP26H is purified by passing through basic alumina column instead of dialysis<sup>19</sup>.



**Scheme 1** Preparation strategy of PR-based multiblock copolymers via twice ATRP.

Nowadays using ATRP of hydrophobic vinyl monomers to end-cap CD-based PPRs into PRs remains a challenge<sup>25</sup>. Owing to its high charge density as well as long side chain group with a huge cross-sectional area relative to the inner cavity of  $\gamma$ -CDs, a hydrophilic, ionic and biocompatible vinyl monomer MPC is expected to have a low competing inclusion ability with  $\gamma$ -CDs to validly attenuate the unpleasant split-off of threaded  $\gamma$ -CDs from non end-capped polymeric axes during the further ATRP<sup>26,27</sup>. So in the second ATRP, MPC is chosen as an end-capping monomer and Cu(I)Br/Me<sub>6</sub>TREN as catalyst to converse  $\gamma$ -CD/PHEMA-PPO-PEO-PPO-PHEMA PPRs into PRs. The composition and yields are summarized in Table 1 (See more information in Preparation and Scheme S1 of Supporting Information). For the convenience, the resulting PR-based multiblock copolymers are assigned as PEP26HxCDyM, where x represents the feed molar ratio of  $\gamma$ -CD to PEP26H and y stands for that of MPC to PEP26H, respectively.

**Table 1** Composition, yield and peak maximum of GPC traces for PR-based multiblock copolymers

Entry	Molar ratio of PEP26H: $\gamma$ -CD:MPC		Yield <sup>b</sup> (%)	Peak Maximum <sup>c</sup> /min
	Feed ratio	Found ratio <sup>a</sup>		
PEP26H29CD28M	1:29:28	1:12.3:23.1	41.9	17.72
PEP26H29CD42M	1:29:42	1:8.3:36.6	43.3	17.61
PEP26H29CD70M	1:29:70	1:11.8:65.8	49.8	17.40
PEP26H29CD98M	1:29:98	1:10.1:100.0	57.8	17.00
PEP26H16CD70M	1:16:70	1:4.5:67.2	52.3	17.47
PEP26H0CD98M	1:0:98	1:0:93.3	84.5	17.31

<sup>a</sup> Determined by <sup>1</sup>H NMR analysis (Figure S1 & S2) in DMSO-d<sub>6</sub>/D<sub>2</sub>O (1:1, v/v)

<sup>b</sup> Calculated based on the weight of collected PR divided by that of all starting materials

<sup>c</sup> Determined from GPC traces of PEP26HxCDyM

As can be seen, the found molar ratios of  $\gamma$ -CD to PEP26H vary in a range of 8.3-12.3 with the feed molar ratio keeping at 29 after the second ATRP. Also taking account of the data at a feed

molar ratio of 16, about one third added  $\gamma$ -CDs are still entrapped on the pentablock copolymer backbones, suggesting the relatively weak competing inclusion complexation of  $\gamma$ -CDs with MPC as compared to other hydrophobic vinyl monomers, such as butyl methacrylate, 2-(diethylamino)ethyl methacrylate, etc., which are found to extract nearly all the threaded  $\gamma$ -CDs from the PEP26H before the second ATRP initiation at the same feed molar ratios. However, the DPs of PMPC segments for all the copolymers including PEP26H0CD98 match the feed molar ratio of MPC to PEP26H, revealed that the macroinitiators in the form of PPRs indeed possess a very high chain end functionality and initiating efficiency in the second ATRP. Furthermore, the mild yields in a range of 41.9-57.8 % are arisen from the slipping off of around two third added  $\gamma$ -CDs. Even so, these yields are markedly higher than those ever reported loose-fit and/or over-fit structured  $\gamma$ -CD-based PRs<sup>11,23</sup>.

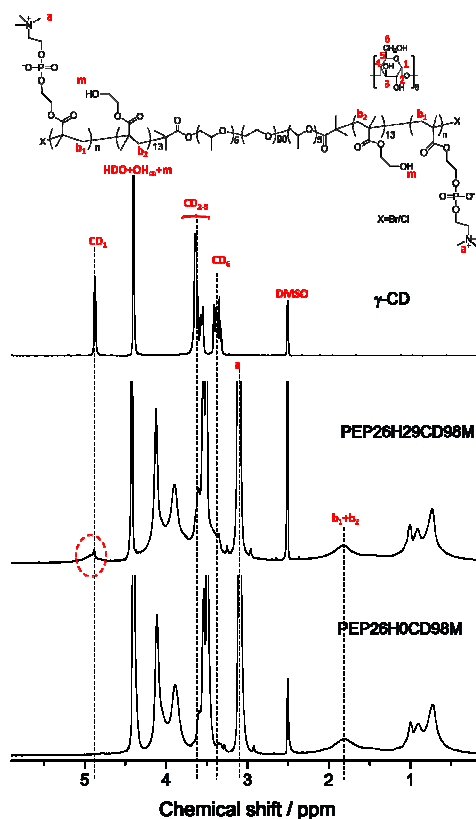


**Fig. 1** <sup>1</sup>H NMR spectra of  $\gamma$ -CD, PEP26H29CD98M and PEP26H0CD98M in DMSO-d<sub>6</sub>/D<sub>2</sub>O (1:1, v/v) at 25 °C.

The <sup>1</sup>H NMR spectra provide direct evidence to confirm the preparation of single-chain stranded  $\gamma$ -CD-based PRs. As can be seen in Figure 1, all typical proton resonance peaks of both  $\gamma$ -CD and blank PEP26H0CD98M copolymer appear in the spectrum of PEP26H29CD98M. Especially, the proton resonance peak (CD<sub>1</sub>) of  $\gamma$ -CD in the PR is clearly broader as compared with free  $\gamma$ -CD due to the decrease of conformational flexibility of  $\gamma$ -CD along the polymer main chain upon the PR formation.

The GPC traces of  $\gamma$ -CD, PEP26H and PRs are presented in Figure 2 and Figure S3, respectively. According to previous reports<sup>17</sup>, DMSO or DMF with a low concentration of LiBr is usually utilized as extraction solvent for PRs. However, as the

PMPC blocks in the PRs are insoluble in DMF in this study<sup>28</sup>, a mixture of DMF/H<sub>2</sub>O (1:1, v/v) is used as a co-eluent solvent for the GPC analysis. Because PS standards routinely used for calibrating GPC data are not soluble in such mixed solvent of DMF/H<sub>2</sub>O, the measurement results of molecular weight and molecular weight distribution are not included in Table 1. However, all the GPC traces exhibit a nearly symmetrical singlet peak with a shift to a shorter retention time in the peak maximum value with the increasing of feed molar ratio of MPC or  $\gamma$ -CD to PEP26H as compared with PEP26H<sup>29</sup>, indicating the successful preparation of PR-based multiblock copolymers by a twice ATRP protocol. What's more, the absence of  $\gamma$ -CD peak within the GPC traces of all the PR samples testifies the fact that no free  $\gamma$ -CD is left in the PR samples after the purification<sup>30</sup>. As a result, the characteristic peaks of  $\gamma$ -CD appeared in the <sup>1</sup>H NMR spectra of the resulting PR samples undeniably declare the presence of threaded and end-capped  $\gamma$ -CDs onto the polymeric main chain<sup>8</sup>, which is also supported by the difference in the peak maximum values between PEP26H0CD98M and PEP26H29CD98M as shown in Figure S4.

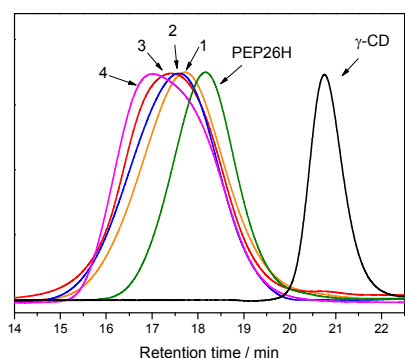


**Fig. 2** GPC traces of  $\gamma$ -CD, PEP26H, PEP26H29CD28M (1), PEP26H29CD42M (2), PEP26H29CD70M (3) and PEP26H29CD98M (4) using a mixture of DMF/H<sub>2</sub>O (10 mmol/L LiBr) (1:1, v/v) as an eluent at 30 °C.

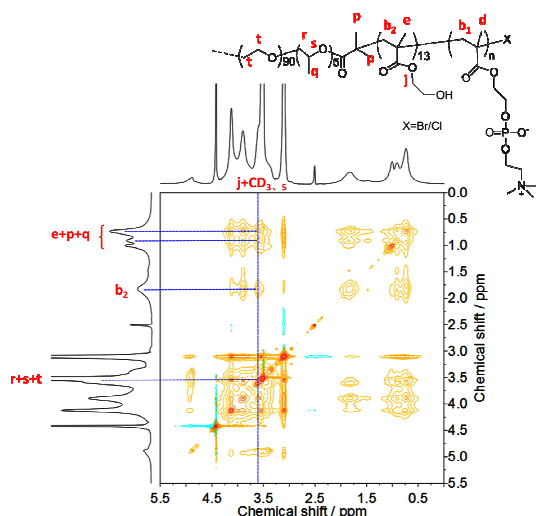


**Fig. 3** 2D-NOESY NMR spectrum of PEP26H29CD98M in DMSO-d<sub>6</sub>/D<sub>2</sub>O (1:1, v/v) at 25 °C.

2D-NOESY NMR correlation analysis is a powerful technique to explore supramolecular structure between host and guest molecules in polyrotaxanes<sup>31</sup>. As outlined in the 2D-NOESY NMR

spectrum of PEP26H29CD98M (Figure 3), the CD<sub>3</sub> and CD<sub>5</sub> protons of  $\gamma$ -CD, which are sited inside the CD cavity, clearly correlate with not only the methylene (H<sub>b2</sub>) and  $\alpha$ -methyl (H<sub>e</sub>) protons of PHEMA chain and other methyl protons (H<sub>p</sub>, H<sub>q</sub>), but also the methylene (H<sub>i</sub>) protons of PEO chain and the methylene (H<sub>r</sub>) and methine (H<sub>s</sub>) protons of PPO short chain. It is also noteworthy that, despite the chemical shifts overlap with CD<sub>3</sub> and CD<sub>5</sub> protons of  $\gamma$ -CD in the <sup>1</sup>H NMR spectrum, the above-mentioned correlations could not be originated from the CD<sub>2</sub> and CD<sub>4</sub> protons, which are located outside the CD cavity, because of the extinction of free  $\gamma$ -CD as shown in its GPC curve in Figure 2. Similar correlations also occur in other PEP26HxCdYm samples (Figure S5). So it is reasonable to conclude that some end-capped  $\gamma$ -CDs slip from flanked PHEMA to the middle PEO block to form a novel polyrotaxane with mixed over-fit (with PHEMA region) and loose-fit (with PEO region) conformations in a way of head-head or tail-tail as schematically described in Scheme 1.

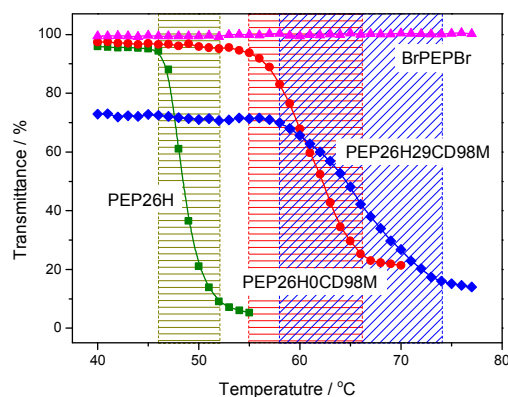


**Fig. 4** Turbidity measurement data obtained from aqueous solutions (0.5%, w/w) of BrPEPBr ( $\blacktriangle$ ), PEP26H ( $\blacksquare$ ), PEP26H0CD98M ( $\bullet$ ) and PEP26H29CD98M ( $\blacklozenge$ ) (Striped rectangle zones represent relevant phase transition ranges, respectively).

In comparison to the cross-sectional area of PPO and PDMS, the PHEMA chains are thicker and PEG chain is thinner. As a consequence, the  $\gamma$ -CDs are threaded onto PHEMA to form the over-fit and are entrapped on PEG to give rise to the loose-fit structured PR-based multiblock copolymers after the second ATRP of MPC. However, both the structures are not characteristic of the channel-like crystal structure as observed in the tight-fit PPRs or PRs formed from PPO or PDMS with  $\gamma$ -CDs<sup>14</sup>. The motility of  $\gamma$ -CDs dynamically entrapped on the PHEMA-PPO-PEO-PPO-PHEMA chain is demonstrated by turbidity measurements as shown in Figure 4. BrPEPBr expresses a nearly 100 % transmittance without any detectable phase transition in the tested temperature scope due to its perfect hydrophilicity, a character very similar to PEG<sup>32</sup>. However, to attach PHEMA brings in an inverse temperature-responsive behaviour to PEP26H with a low cloud point (CP) appeared at 48.4 °C and a narrow phase transition range ( $\Delta T$ ) of 6 °C seen as previously reported by Weaver *et al.*<sup>33</sup>. In contrast, PEP26H0CD98M presents a broad phase transition range ( $\Delta T$  = 11 °C) at a higher temperature zone (CP = 60.7 °C) as a result of attaching water-soluble PMPC blocks. As for PEP26H29CD98M, those  $\gamma$ -CDs distributed on the middle



pentablock polymeric axle can further buffer the aggregation of PHEMA blocks in response to the environmental temperature rise, showing great potential as a kind of novel molecular dampers, leading to the emergence of highest CP (65.8 °C) and broadest  $\Delta T$  (16 °C). To the best of our knowledge, this is the first report of single-chain stranded  $\gamma$ -CD/ PMPC-PHEMA-PPO-PEO-PPO-PHEMA-PMPC PRs with such unique stimuli-responsibility and damping effect. The mild transmittance (~74 %) at 40 °C of this sample rather than ~96 % for PEP26H0CD98M also verifies the favourable entrapping of  $\gamma$ -CDs on the PR main chain holding both loose- and over-fit archi-tecture.

The single-chain stranded over-fit and loose-fit structure of the resulting PRs are also supported by WXR D analyses as shown in Figure 5, although they exhibit no such characteristic channel-like crystal structure stemmed from the tight-fit structured PPRs or PRs. Different from cage-type crystal  $\gamma$ -CD and PEP26H, the latter of which displays acute characteristic diffraction peaks of crystalline PEO<sup>7</sup>, PEP26H0CD98M just displays single broad diffraction peak centered at  $2\theta$  of 19.1 °, indicating that the hepta-block copolymer with high polar PMPC segments is apt to take an irregular noncrystalline state. However, for the PR sample PEP26H29CD98M, those dynamically entrapped  $\gamma$ -CDs would disarrange the inter/intramolecular topological structure to a higher chaos state, shifting the featured single broad diffraction peak to smaller  $2\theta$  of 17.6 °, as suggested by Bragg's Law<sup>34</sup>.

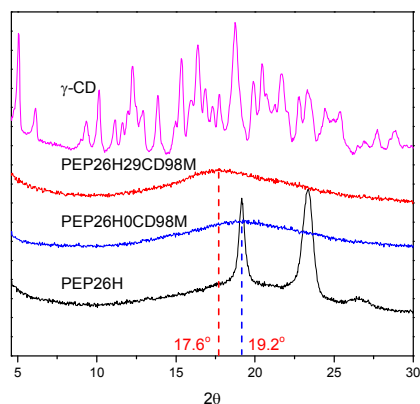


Fig. 5 WXR D patterns of  $\gamma$ -CD, PEP26H, PEP26H0CD98M and PEP26H29CD98M.

TGA analyses are also performed on the samples  $\gamma$ -CD, PEP26H, PEP26H0CD98M and PEP26H29CD98M in the range of 150 °C to 550 °C as depicted in Figure S6. The higher residual weight ratio (>30 %) of PEP26H29CD98M at 550 °C clearly shows the same residual thermo-stable components with PEP26H0CD98M arisen from the phosphorylcholine moieties of end-capped PMPC blocks, further suggesting the undertaking of second ATRP of MPC, well in agreement with the GPC results. Due to the thermal decomposition of PHEMA-PPO-PEO-PPO-PHEMA, the samples PEP26H and PEP26H0CD98M reveal the same initial temperature of thermal weight loss at 220 °C besides the difference in breakdown speed afterwards. On the contrary, PEP26H29CD98M starts to decompose at 195 °C, proclaiming the occurrence of extra irregularity in the aggregation state structure of the middle pentablock probably exerted by random-distributed, threaded and moveable  $\gamma$ -CDs. Significantly, similar to pure  $\gamma$ -CD, it also decomposes at a faster rate in 310~350 °C relative to those of

naked PEP26H and PEP26H0CD98M. This provides evidence supporting the formation of simultaneously loose-fit and over-fit structured PR-based multiblock copolymers in which  $\gamma$ -CDs are bound to the middle PHEMA-PPO-PEO-PPO-PHEMA axle.

In general FTIR acts as a useful tool to prove the existence of both guest and host molecules in their inclusion complexes<sup>35</sup>. Figure S7 portrays the FTIR spectra of  $\gamma$ -CD, PEP26H, PEP26H0CD98M, PEP26H29CD98M and PEP26H29CD42M, respectively. The spectra of the PMPC block containing samples exhibit distinct featured peaks of MPC unit at 788  $\text{cm}^{-1}$  (P-O-CH<sub>2</sub> stretching vibration) and 1088  $\text{cm}^{-1}$  (CH<sub>2</sub>-N-CH<sub>3</sub> stretching vibration)<sup>36</sup>. Besides those two characteristic vibrations, FTIR band frequencies of the two PR samples tested at 1028  $\text{cm}^{-1}$  and 584  $\text{cm}^{-1}$  are registered as bend vibration of O-H in  $\gamma$ -CDs and the pyranose ring pulsation vibration, respectively<sup>37,38</sup>. Moreover, the absorption bands of pyranose ring pulsation vibrations are slightly broadened for the formation of inclusion complexes, similar to the case observed by Roik *et al.*<sup>39</sup>. The results forcefully assert the successful preparation of the alleged single-chain stranded loose- and over-fit structured PR-based multiblock copolymers in this study.

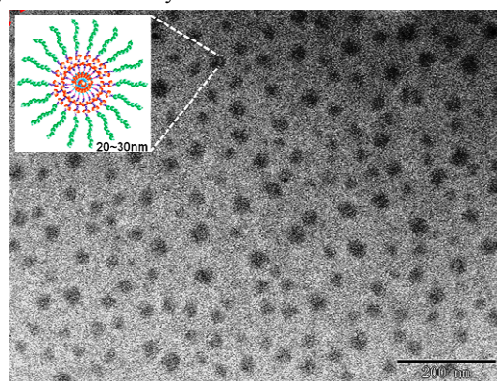


Fig. 6 TEM image of PEP26H29CD98M aggregates.

As a typical sample of the PR-based multiblock copolymers, the self-aggregation behavior of PEP26H29CD98M is observed by TEM. Attaching the hydrophilic and ionic PMPC oligomers to two ends of  $\gamma$ -CD/PHEMA-PPO-PEO-PPO-PHEMA PPR using ATRP induces the copolymers to self-assemble into the unique core-shell structured micelles as illustrated in Figure 6. Here the middle pentablock segments entrapped by  $\gamma$ -CDs possess a relatively weak water-solubility to function in a way analogous to hydrophobic core, while those flanking PMPC chains prefer to array in order as hydrophilic outer shell in aqueous solution. As can be seen, the diameter of these spherical micelles is in a range of 20-30 nm. These particles are very suitable to be used as carriers for the drug controlled release<sup>40,41</sup>. Furthermore, such PRs remain abundant room in  $\gamma$ -CD cavities for additional drug inclusion. So they are promising candidates for the drug controlled release applications<sup>42,43</sup>.

## Conclusions

PPRs constructed from the self-assembly of  $\gamma$ -CDs with bromide terminated PHEMA-PPO-PEO-PPO-PHEMA are end-capped by further using ATRP of MPC to converse into water-soluble

single-chain stranded PR-based multiblock copolymers simultaneously showing the loose-fit and over-fit inclusion complex structure in yields of 41.9-57.8 %. About one third added  $\gamma$ -CDs are still entrapped on the polymer main chain after the second ATRP. The DP of attached PMPC segments matches the feed molar ratio of MPC to macroinitiator. The unique loose-fit and over-fit architectures are demonstrated by 2D-NOESY NMR correlations, turbidity measurement data and TGA and WXRD analyses.

## Notes and references

<sup>a</sup> School of Materials Science and Engineering, Beijing Institute of Technology, Beijing 100081, China. Fax: 86-01-68912650; Tel: 86-01-68912650; E-mail: sainfeng@bit.edu.cn

1. F. Huang and H. W. Gibson, *Progress in Polymer Science*, 2005, **30**, 982-1018.
2. J. H. Seo, S. Kakinoki, Y. Inoue, T. Yamaoka, K. Ishihara and N. Yui, *Journal of the American Chemical Society*, 2013, **135**, 5513-5516.
3. B. L. Tardy, H. H. Dam, M. M. Kamphuis, J. J. Richardson and F. Caruso, *Biomacromolecules*, 2014, **15**, 53-59.
4. K. Kato, T. Yasuda and K. Ito, *Macromolecules*, 2013, **46**, 310-316.
5. J. Wu and C. Gao, *Macromolecules*, 2010, **43**, 7139-7146.
6. A. Harada, A. Hashidzume, H. Yamaguchi and Y. Takashima, *Chemical Reviews*, 2009, **109**, 5974-6023.
7. A. Harada, A. Hashidzume and Y. Takashima, *Advances in Polymer Science*, 2006, **201**, 1-43.
8. M. Okada, Y. Takashima and A. Harada, *Macromolecules*, 2004, **37**, 7075-7077.
9. A. Harada, J. Li and M. Kamachi, *Nature*, 1994, **370**, 126-128.
10. A. Harada, T. Nishiyama, Y. Kawaguchi, M. Okada and M. Kamachi, *Macromolecules*, 1997, **30**, 7115-7118.
11. A. Takahashi, R. Katoono and N. Yui, *Macromolecules*, 2009, **42**, 8587-8589.
12. T. Miura, T. Kida and M. Akashi, *Macromolecules*, 2011, **44**, 3723-3729.
13. J. Wang, S. Li, L. Ye, A. Y. Zhang and Z. G. Feng, *Macromolecular Rapid Communications*, 2012, **33**, 1143-1148.
14. H. Okumura, Y. Kawaguchi and A. Harada, *Macromolecules*, 2001, **34**, 6338-6343.
15. A. Harada, M. Okada, J. Li and M. Kamachi, *Macromolecules*, 1995, **28**, 8406-8411.
16. L. Ren, F. Ke, Y. Chen, D. Liang and J. Huang, *Macromolecules*, 2008, **41**, 5295-5300.
17. X. Tong, X. Zhang, L. Ye, A. Y. Zhang and Z. G. Feng, *Polymer*, 2008, **49**, 4489-4493.
18. X. Zhang, X. Zhu, F. Ke, L. Ye, E. Q. Chen, A. Y. Zhang and Z. G. Feng, *Polymer*, 2009, **50**, 4343-4351.
19. T. Kong, L. Ye, A. Y. Zhang and Z. G. Feng, *Beilstein journal of organic chemistry*, 2014, **10**, 2461-2469.
20. X. Jin, Y. Shen and S. Zhu, *Macromolecular Materials and Engineering*, 2003, **288**, 925-935.
21. P. Gao, P. Wang, X. Geng, L. Ye, A. Zhang and Z. Feng, *Acta Chimica Sinica*, 2013, **71**, 347-350.
22. W. Huang, J.-B. Kim, M. L. Bruening and G. L. Baker, *Macromolecules*, 2002, **35**, 1175-1179.
23. L. Jiang, L. Ye, A. Y. Zhang and Z. G. Feng, *Macromolecular Chemistry and Physics*, 2014, **215**, 1022-1029.
24. B. M. Rosen and V. Percec, *Chemical Reviews*, 2009, **109**, 5069-5119.
25. S. Bernhardt, P. Gloickner, A. Theis and H. Ritter, *Macromolecules*, 2011, **34**, 1647-1649.
26. A. Harada, *Coordination Chemistry Reviews*, 1996, **148**, 115-133.
27. H. S. Choi, T. Ooya, S. C. Lee, S. Sasaki, M. Kurisawa, H. Uyama and N. Yui, *Macromolecules*, 2004, **37**, 6705-6710.
28. M. Jiani, G. Ming, Y. Shan, Z. Shiping and G. Yongkuan, *Progress in Chemistry*, 2008, **20**, 1151-1157.
29. M. Jbeily, T. Naolou, M. Bilal, E. Amado and J. Kressler, *Polymer International*, 2014, **63**, 894-901.
30. J. Wang, P. Gao, L. Ye, A. Y. Zhang and Z. G. Feng, *The Journal of Physical Chemistry B*, 2010, **114**, 5342-5349.
31. A. Harada, *Advances in Polymer Science*, 1997, **133**, 141-191.
32. J. F. Lutz, *Journal of Polymer Science Part A: Polymer Chemistry*, 2008, **46**, 3459-3470.
33. J. V. M. Weaver, I. Bannister, K. L. Robinson, X. Bories-Azeau and S. P. Armes, *Macromolecules*, 2004, **37**, 2395-2403.
34. J. Gao, S. Yu, B. Zheng, Q. Song, X. Peng, Y. Lin, G. Zou and Q. Zhang, *RSC Advances*, 2014, **4**, 36675.
35. H. Jiao, S. H. Goh and S. Valiyaveetil, *Macromolecules*, 2001, **34**, 8138-8142.
36. D. Xiong, Y. Deng, N. Wang and Y. Yang, *Applied Surface Science*, 2014, **298**, 56-61.
37. X. Chen, R. Chen, Z. Guo, C. Li and P. Li, *Food Chemistry*, 2007, **101**, 1580-1584.
38. M. Raileanu, L. Todan, M. Crisan, A. Braileanu, A. Rusu, C. Bradu, A. Carpov and M. Zaharescu, *Journal of Environmental Protection*, 2010, **1**, 302-313.
39. N. V. Roik and L. A. Belyakova, *Physics and Chemistry of Solid State*, 2011, **12**, 168-173.
40. L. Jiang, Z. M. Gao, L. Ye, A. Y. Zhang and Z. G. Feng, *Polymer*, 2013, **54**, 5188-5198.
41. L. Jiang, Z. M. Gao, L. Ye, A. Y. Zhang and Z. G. Feng, *Biomaterials Science*, 2013, **1**, 1282-1291.
42. S. Tan, K. Ladewig, Q. Fu, A. Blencowe and G. G. Qiao, *Macromolecular Rapid Communications*, 2014, **35**, 1166-1184.
43. B. Han, X. Liao and B. Yang, *Progress in Chemistry*, 2014, **26**, 1039-1049.